

# Near-Nyquist optical pulse generation with fiber optical parametric amplification

Armand Vedadi,\* Mohammad Amin Shoaie, and Camille-Sophie Brès

Photonic Systems Laboratory (PHOSL), STI-IEL, EPFL, CH-1015 Lausanne, Switzerland

\*[armand.vedadi@epfl.ch](mailto:armand.vedadi@epfl.ch)

**Abstract:** A novel method using optical fiber parametric amplification and phase modulation is proposed in order to generate Nyquist pulses. Using parabolic pulses as a pump, we show theoretically that it is possible to generate Nyquist pulses. Furthermore, we show that by using a sinusoidal pump (pump intensity modulated by an RF tone), it is possible to obtain pulses with characteristics that are close to Nyquist limited pulses. We demonstrate experimentally the generation of bandwidth limited pulses with full width half maximum of 14 ps at 10 GHz repetition rate. We also discuss limitations of this method and means to overcome these limitations.

©2012 Optical Society of America

**OCIS codes:** (060.4370) Nonlinear optics, fibers; (190.4970) Parametric oscillators and amplifiers.

---

## References and links

1. R. Essiambre, G. Kramer, P. Winzer, G. Foschini, and B. Goebel, "Capacity limits of optical fiber networks," *J. Lightwave Technol.* **28**(4), 662–701 (2010).
2. G. Bosco, A. Carena, V. Curri, P. Poggiolini, and F. Forghieri, "Performance limits of Nyquist-WDM and CO-OFDM in high-speed PM-QPSK systems," *IEEE Photon. Technol. Lett.* **22**(15), 1129–1131 (2010).
3. R. Schmogrow, M. Winter, M. Meyer, D. Hillerkuss, S. Wolf, B. Baeuerle, A. Ludwig, B. Nebendahl, S. Ben-Ezra, J. Meyer, M. Dreschmann, M. Huebner, J. Becker, C. Koos, W. Freude, and J. Leuthold, "Real-time Nyquist pulse generation beyond 100 Gbit/s and its relation to OFDM," *Opt. Express* **20**(1), 317–337 (2012).
4. A. Wiberg, L. Liu, Z. Tong, E. Myslivets, V. Ataie, N. Alic, and S. Radic, "Cavity-less pulse source based optical sampled ADC," in European Conference and Exhibition on Optical Communication ECOC 2012, OSA Technical Digest (online) (Optical Society of America, 2012), paper Mo.2.A.3.
5. M. Nakazawa, T. Hirooka, P. Ruan, and P. Guan, "Ultrahigh-speed "orthogonal" TDM transmission with an optical Nyquist pulse train," *Opt. Express* **20**(2), 1129–1140 (2012).
6. A. Vedadi, A. Ariaei, M. Jadidi, and J. Salehi, "Theoretical study of high repetition rate short pulse generation with fiber optical parametric amplification," *J. Lightwave Technol.* **30**(9), 1263–1268 (2012).
7. A. A. Vedadi, M. A. Shoaie, and C.-S. Brès, "Experimental investigation of pulse generation with one-pump fiber optical parametric amplification," *Opt. Express* **20**(24), 27344–27354 (2012).
8. A. Vedadi, M. Shoaie, and C. Brès, "Near Nyquist sinc optical pulse generation with fiber optical parametric amplification," in European Conference and Exhibition on Optical Communication ECOC 2012, OSA Technical Digest (online) (Optical Society of America, 2012), paper P1.02.
9. C. Finot, L. Provost, P. Petropoulos, and D. J. Richardson, "Parabolic pulse generation through passive nonlinear pulse reshaping in a normally dispersive two segment fiber device," *Opt. Express* **15**(3), 852–864 (2007).

---

## 1. Introduction

With growing needs for end user bandwidth, the demand for higher capacity optical fiber networks is rapidly rising. The lack of viable alternatives to expand the bandwidth of optical telecommunications beyond the limitations imposed by erbium doped fiber amplifiers (EDFAs) has funneled recent research efforts towards increasing the spectral efficiency of transmitted signals. Besides multiplying the number of transmitted bits per symbol with multi-level phase and/or amplitude modulation schemes in coherent transmission systems, efforts are underway to contain the transmitted signal spectrum within a bandwidth that is as close as possible to the symbol rate, which is the lower bound dictated by the Nyquist theorem [1].

Such trend is observed in recent demonstrations of Nyquist-WDM transmissions [2, 3]. In these schemes, the symbol pulse is fabricated so that its spectrum has a near rectangular shape. Each channel spectrum is therefore contained within a bandwidth that is close to the

Nyquist limit. Hence a shorter guard band is needed and channels may be located closer to each other, increasing the overall transmission spectral efficiency. Such spectral shaping can be obtained by optical filtering or by digital signal processing techniques. The former is however limited by the steepness of the optical filter used while the latter is limited by the electronic bandwidth [2, 3]. Moreover, in applications like sampling and optical analog to digital converters (ADC), being able to employ an optical Nyquist-limited pulse to sample the data could significantly ease constraints on bandwidth [4]. In [5], an “orthogonal” time division multiplexing (TDM) was performed using Nyquist pulse train. The pulses were obtained all-optically using a mode-locked laser and a spatial modulator.

In recent works [6, 7], it was shown theoretically and experimentally that it is possible to achieve approximate sinc shaped pulses using fiber optical parametric amplifiers (FOPAs) in a cavity-free configuration. Indeed, an intensity-modulated pump coupled with a CW seed (signal) inside a highly nonlinear fiber (HNLF) will generate an idler wave which envelope is compressed compared to that of the pump. However, during the process of pulse generation, the pump also induces a linear chirp, which results in the spreading and distortion of the pulse’s spectrum. In [8], we have shown that the pump-induced chirp can be compensated with a phase modulator and demonstrated the all-optical generation of a bandwidth-contained pulse that nears characteristics of a Nyquist pulse from a sinusoidally driven single pump FOPA. This all-optical source alleviates the limitations imposed by the electrical bandwidth and/or the steepness of optical filters. The cavity-free architecture allows for more stability and flexibility at any frequency rate since there is no need to maintain phase-locking.

In this work, this approach is studied in depth theoretically and experimentally. We show that with proper design, it is possible to generate near-Nyquist pulses that can have potential applications in “orthogonal” TDM, WDM-Nyquist transmissions and optical detection/sampling. We also point out the limitations of this approach.

## 2. Theory and numerical simulations

### 2.1. Principle of generation of near-Nyquist pulses using a sinusoidal pump

The principle of pulse generation through FOPA is depicted in Fig. 1. A high power pump at angular frequency  $\omega_p$  is coupled with a low power signal at  $\omega_s$  and injected into an optical fiber. Through four-wave mixing (FWM), a new idler wave will be generated at a frequency  $\omega_i$  that is symmetrical to  $\omega_s$  with respect to  $\omega_p$ , such that  $\omega_s - \omega_p = \omega_p - \omega_i = \Delta\omega_s$ . Suppose that the pump is intensity-modulated by a sinusoid such that  $A_p(0, t) = \sqrt{P_0} \cos(\pi f_R t)$ , where  $P_0$  is the pump peak power and  $f_R$  is the pump repetition rate. Because the Kerr process on which FWM is based has a quasi-instantaneous response, the generated idler at the fiber output has a pulse shape that is compressed compared to the pump. The pulse width depends on the linear phase mismatch  $\Delta\beta_L$  between the pump, idler and signal waves [6, 7]. In particular, when:

$$\Delta\beta_L \triangleq \beta_2 \Delta\omega_s^2 + \frac{\beta_4}{12} \Delta\omega_s^4 = -4\gamma P_0 \quad (1)$$

where  $\beta_2$  and  $\beta_4$  are the amplifying fiber dispersion and dispersion curve, then the idler at the FOPA output will have the following wave amplitude [5]:

$$A_i(\tau) \approx j \left( \sqrt{P_s} \gamma P_0 L \right) \text{sinc}(2\pi\gamma P_0 L f_R \tau) \times e^{j \left( \gamma P_0 \cos^2(\pi f_R t) + \frac{\beta_3}{6} \Delta\omega_s \right) L} \quad (2)$$

$\gamma$  is the nonlinear coefficient of the amplifying fiber and  $\beta_3$  is the fiber dispersion slope. Equation (2) shows that the pump induces a chirp on the generated idler. This chirp leads to a spreading of the pulse spectrum, which limits their usefulness for WDM-Nyquist transmissions. Unlike Gaussian pulses, this chirp cannot be straightforwardly compensated by

a passive dispersive medium. Rather, an active chirp-compensating module is required. Noting that  $\cos^2(\pi f_R t) = [1 + \cos(2\pi f_R t)]/2$ , we use a phase modulator driven by an RF synthesizer at  $f_R$  to compensate for the chirp. The principle is shown in Fig. 1. Before the phase modulator, the generated idler at the FOPA output is chirped and hence its spectrum is spread. Driving the phase modulator with the sinusoidal pattern  $\frac{\gamma P_0 L}{2} \cos(2\pi f_R t)$ , it is possible to suppress completely the FOPA induced chirp on the idler by aligning the peak of the generated pulse with the trough of the driving sinusoid. In the ideal case, the idler optical spectrum after chirp compensation must be close to a rectangle of width  $2\gamma P_0 L$ . Note that using a phase modulator one can exactly compensate the induced chirp.

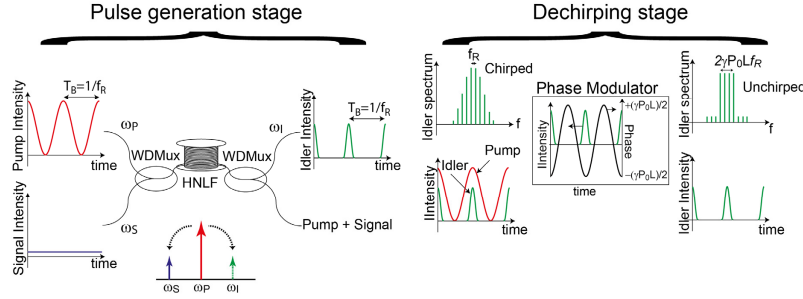


Fig. 1. Principle of near-Nyquist pulse generation with fiber optical parametric amplification and a subsequent phase modulator for dechirping. WDMux: Wavelength Division Multiplexer.

## 2.2. Comparison between sinusoidal and parabolic pumping

In obtaining Eq. (2), we assumed that  $P_p(0, t) \approx P_0(1 - (\pi f_R t)^2)$  in the vicinity of the pump peak power [6, 7]. Moreover, we neglected terms that are of higher orders than  $t$ . Hence, the pulse that is generated on the idler side is approximated by a sinc function. In this section, we discuss the validity of this approximation. In recent years, it has been demonstrated that it is possible to generate parabolic pulses [9]. We assume a parabolic pump such that:

$$P_p(0, t) = \begin{cases} P_0 \{1 - [\pi f_R (t - N)]^2\} & t \in [-1/(\pi f_R), 1/(\pi f_R)] + N/(\pi f_R) \\ 0 & t \notin [-1/(\pi f_R), 1/(\pi f_R)] + N/(\pi f_R) \end{cases} \quad (N \in \mathbb{Z}) \quad (3)$$

The shapes of the parabolic pump, together with the corresponding sinusoidal pump are plotted in Fig. 2(a). Using Eq. (3) without making any approximation, we have:

$$A_i(\tau) = \begin{cases} j\sqrt{P_s} \gamma P_0 L (1 - (\pi f_R t)^2) \text{sinc}(2\pi \gamma P_0 L f_R \tau) \times e^{j(\gamma P_0 (1 - (\pi f_R t)^2) + \frac{\beta_3}{6} \Delta \alpha_s)L} & t \in [-1/(\pi f_R), 1/(\pi f_R)] \\ 0 & t \notin [-1/(\pi f_R), 1/(\pi f_R)] \end{cases} \quad (4)$$

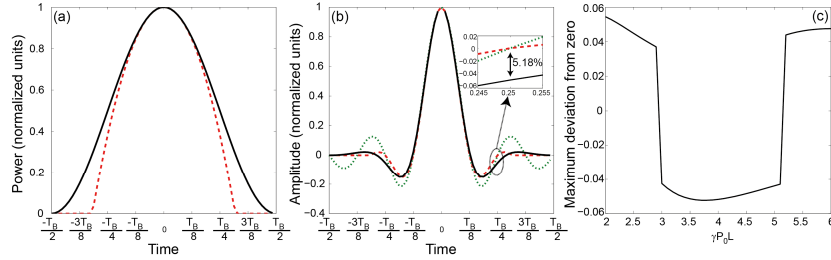


Fig. 2. (a) Sinusoidal pump (solid line) and parabolic pump (dashed line). (b) Idler generated by a sinusoidal pump (solid line), by a parabolic pump (dashed line) and sinc shaped pulse (dotted line). (c) Maximum idler amplitude at the Nyquist pulse zeroes.  $T_B$  corresponds to one bit duration ( $T_B = 1/f_R$ ).

In Eq. (4), we have restrained ourselves, without loss of generality, to the time interval  $[-1/f_R, 1/f_R]$ . Equation (4) shows that although the generated pulse is not a perfect sinc, it remains a Nyquist pulse in the time domain. In [4], it was shown that for  $\gamma P_0 L > 2$ , the sinc function is a very good approximation of the pulse shape. Figure 2(b) shows the generated pulse envelope using sinusoidal pumping and parametric pumping for  $\gamma P_0 L = 4$ . This corresponds to a peak gain of 12.3 dB at the signal location. The corresponding sinc pulse from Eq. (2) is also shown. The main lobe of the three pulses fit well with each other. In particular, the positions of the nearest zeros to the pulses peak are the same (at  $-T_B/8$  and  $T_B/8$ ). The pulse generated by the sinusoidal pump however does not cross the zero ordinate at  $t = \pm T_B/4$  and  $t = \pm 3T_B/8$ , which are other locations of the corresponding Nyquist pulses zeroes. The maximum deviation at these points is less than 5.2%, which can induce an inter-symbol crosstalk lower than  $-12.8$  dB for orthogonal TDM. Figure 2(c) summarizes, as a function of  $\gamma P_0 L$ , the maximum deviation at the Nyquist pulses zeros location of a pulse generated with a sinusoidal pump. The maximum inter-symbol crosstalk is below  $-12.6$  dB (5.45%). Equation (4) also shows that a gating occurs in the time domain for pulses generated by a parabolic pump. This can lead, after removal of the chirp, to an aliasing of the spectrum in the frequency domain. In order to assess the impact of that aliasing on the dechirped spectrum, we have calculated the spectra of the unchirped pulses generated by a sinusoidal pump and a parabolic pump, for  $\gamma P_0 L = 4$ . The results are plotted in Figs. 3(a) and 3(b). For comparison, we have also plotted in Fig. 3(c) the spectrum of the corresponding sinc pulse. These figures show that when unchirped, all spectra become contained to a bandwidth that is close to  $2f_R \gamma P_0 L$ . For Nyquist pulses, this bandwidth corresponds to two times the Nyquist frequency. However, we observe that the spectral components, spaced by the repetition frequency, are not equal. Moreover, out of the theoretical Nyquist pulse bandwidth, small spectral components remain, which can lead to inter channel crosstalk in WDM-Nyquist transmissions. These features are caused by the fact that the pulses are generated over a finite time domain that is inferior or equal to the bit duration. This creates an aliasing in the frequency domain. In order to show this issue, the spectrum of one pulse that is gated over one bit duration is plotted in dashed lines. These spectra are envelopes of the train of pulses spectra, which clearly shows the influence of aliasing. Therefore, in WDM-Nyquist transmissions systems, a guard band between WDM channels is required to avoid inter channel crosstalk. As an example, Fig. 3 shows that for  $\gamma P_0 L = 4$ , in order to have an inter channel crosstalk below  $-17$  dB, the channels must be separated by a guard band of  $f_R \gamma P_0 L$ , which corresponds to the Nyquist frequency. Note that the pulses generated by a sinusoidal

pump exhibit a lower crosstalk, below  $-22$  dB. For a guard band of  $f_R (\gamma P_0 L - 1)$ , the crosstalk remains below  $-15$  dB.

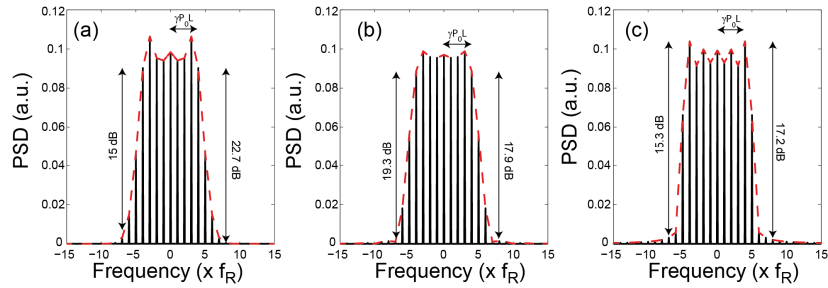


Fig. 3. Spectrum of (a) idler generated by a sinusoidal pump (b) idler generated by a parabolic pump and (c) sinc pulse for  $\gamma P_0 L = 4$ .

For sinc pulses generated in the electrical domain, it is possible to attenuate the aliasing by extensive digital signal processing [2, 3]. However these pulses are limited by the electrical bandwidth.

We summarize below the results of our theoretical investigation of Nyquist and near-Nyquist pulse generation with FOPA:

- The pulses generated by a sinusoidal pump in a FOPA can be assimilated to near-Nyquist pulses, with a maximum inter-symbol crosstalk of less than  $-12.6$  dB for  $\gamma P_0 L = 4$ .
- Using a parabolic pump in a FOPA, it is possible to generate Nyquist pulses.
- When dechirped, all spectra become contained. However, the windowing in the time domain leads to an aliasing that prevents a perfect rectangular chirp and leads to residual inter-channel crosstalk for WDM-Nyquist transmission.

### 3. Experimental setup

The experimental setup is depicted in Fig. 4. For the pump, a continuous wave (CW) laser is intensity modulated by a sinusoid at 10 GHz, then phase modulated by a 10 GHz  $2^{20}$ -1 pseudo random bit sequence (PRBS) in order to suppress stimulated Brillouin backscattering. The pump is then amplified by a booster EDFA and the amplified stimulated emission (ASE) is subsequently filtered by a 2 nm bandwidth filter. A tunable external cavity laser (ECL) is used as a signal. Its power can be adjusted with a variable optical attenuator (VOA). Pump and signal are mixed into a 500 m long highly nonlinear fiber (HNLf) through a wavelength division multiplexer (WDMux). At the output, the idler is isolated from the high power pump and the signal by a WDMux and subsequently phase modulated by the same sinusoid used to drive the pump intensity modulator (IM). RF attenuators and drivers were used to adjust the peak-to-peak voltages of the driving signals in order to ensure that the pump IM is in the linear regime while the idler phase swings between  $\pm \gamma P_0 L / 2$ . A variable optical delay line (VODL) aligns the idler pulses with the trough of the sinusoid.

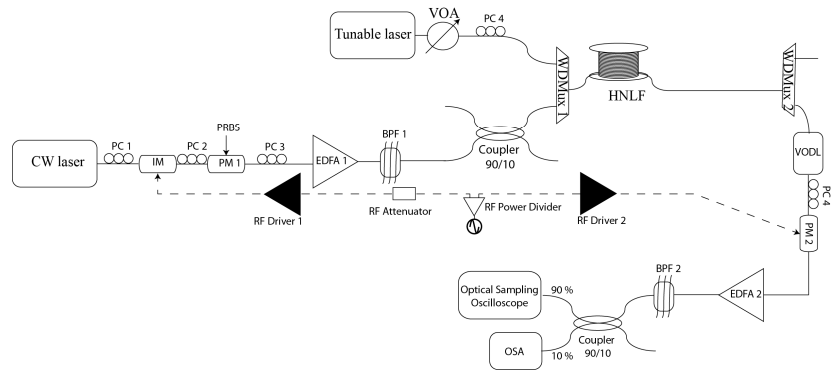


Fig. 4. Experimental Setup. PC: Polarization Controller. EDFA: Erbium Doped Fiber Amplifier. BPF: Bandpass Filter, PM: Phase Modulator, IM: Intensity Modulator, OSA: Optical Spectrum Analyzer.

Before acquisition, the idler is amplified with an EDFA and filtered in order to reach the power threshold of the 500 GHz optical sampling scope. The spectrum was also observed on an optical spectrum analyzer (OSA) with 0.02 nm resolution. This corresponds to 2.5 GHz at 1550 nm, which is sufficient to observe the 10 GHz spaced spectral components.

#### 4. Results and discussions

The pump wavelength in the experiment was set to 1556.1 nm. We used a HNLFF fiber with nonlinear coefficient  $\gamma = 12 \text{ W}^{-1}\text{Km}^{-1}$ , zero dispersion wavelength (ZDW) at 1551 nm and absorption of 0.85 dB/km. The peak pump power was set to 700 mW so as to obtain  $\gamma P_0 L_{eff} = 4$ , where  $L_{eff}$  is the effective length. The signal was located at 1571.8 nm, which corresponds to the edge of the FOPA gain spectrum. Because of energy conservation, the idler was generated at 1540.5 nm. Figures 5(a) and (b) show the idler spectrum before and after chirp compensation. One can observe that the phase modulation reshapes the idler spectrum by growing the amplitude of frequency components near the edge and redistributing energy to the central components. In order to observe that the pulse has a reduced bandwidth, we have plotted in Figs. 5(c) and 5(d) the spectra of the chirped and dechirped pulses in dB scale.

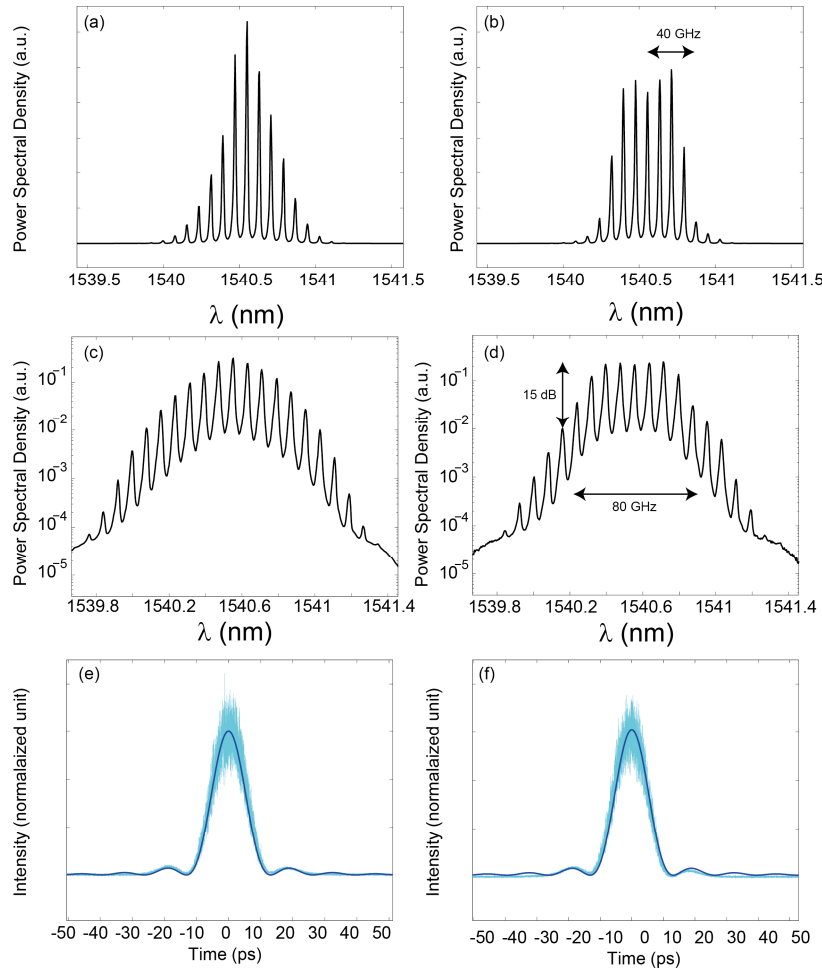


Fig. 5. Spectrum of the idler (a) before phase modulation, (b) after phase modulation, (c) before phase modulation (dB scale), (d) after phase modulation (dB scale). Traces of an idler pulse (e) before phase modulation and (f) after phase modulation.  $\gamma P_0 L = 4$ .

These figures clearly show that the spectrum has been squared, and that most of the energy is contained in an 80 GHz bandwidth, corresponding to 2 times the Nyquist frequency. We also retrieve the fact that an adjacent channel would undergo a crosstalk of less than  $-15$  dB. Using Eq. (2), we expect to get near-sinc pulses of 25 ps width, where the width is defined as the distance between the two zeroes surrounding the main lobe. Note that this corresponds to a full width at half maximum (FWHM) of 14 ps. Figures 5(e) and 5(f) show that the idler temporal trace is not modified after removal of the chirp. We observe a very good fit with the formula given by Eq. (2). Also, the theoretical fit obtained in Fig. 2(b) for a pulse generated by a sinusoidal pump (solid line) is in very good agreement with all measured experimental traces. The generated pulses exhibit an electrical signal to noise ratio (SNR) of 21.5 dB in both cases.

Note that the spectrum of the unchirped pulse is not exactly the same as the one plotted in Fig. 3(a). This is due to the saturation of the RF driver and/or the phase modulator used to compensate for the chirp. Indeed, the peak-to-peak voltage at the phase modulator input must be equal to  $\gamma P_0 L / \pi \times V_\pi$ , where  $V_\pi$  is the voltage required to introduce a phase of  $\pi$  at the phase modulator output. At this value, the RF driver and the phase modulator did not work in the linear regime and as a consequence, the chirp compensation was not ideal. This limitation

could be eliminated by phase modulating the pulse in two subsequent stages. Thus, each phase modulator could be driven with half the voltage and would remain in the linear regime.

In order to verify the influence of the phase modulator and RF driver nonlinearity, we have done the experiment for  $\gamma P_0 L = 3$ , where a lower peak-to-peak voltage is needed to compensate the pump induced chirp. The pump peak power was tuned to 520 mW. The signal was located at 1570.5 nm and the new idler position was at 1541.75 nm. Figures 6(a) and 6(c) show the spectra measured on the OSA before and after phase modulation. They show a clear squaring of the idler spectrum after phase modulation. Likewise the case in Fig. 5, no pulse distortion was observed in the time domain before or after chirp compensation.

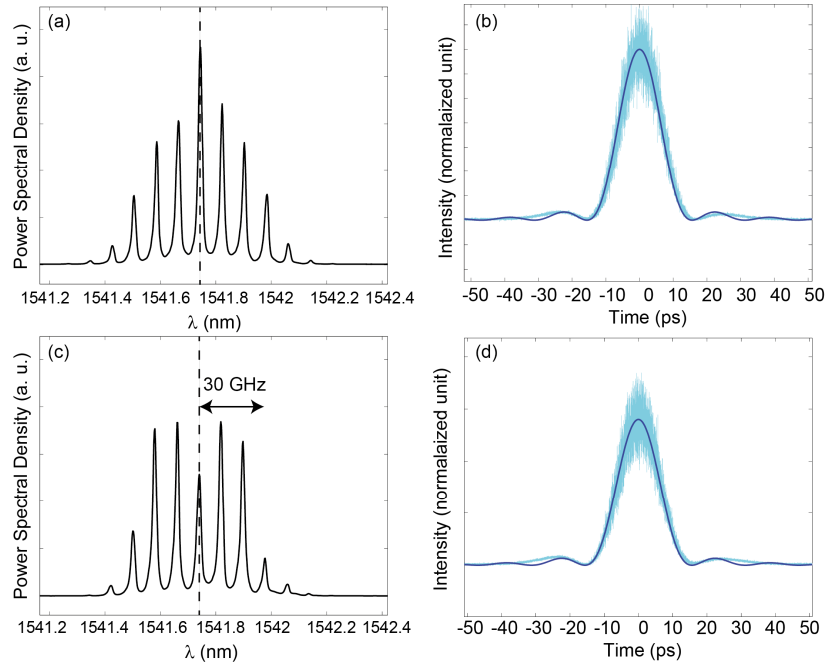


Fig. 6. Spectrum of the idler (a) before phase modulation, (c) after phase modulation. Traces of the idler pulse: (b) before phase modulation and (d) after phase modulation. In all figures:  $\gamma P_0 L = 3$ .

## 5. Conclusion

We have demonstrated a new method to generate near Nyquist pulses using an all-optical and cavity-free configuration. We have shown theoretically that using a sinusoidal pump, the pulses possess characteristics that are close to Nyquist pulses. Moreover, using parabolic pulses, it is possible to obtain Nyquist pulses suitable for “orthogonal” time division multiplexing and WDM Nyquist transmission.

Using a pump modulated by a sinusoid, near Nyquist pulses of 14 ps FWHM were experimentally generated. This scheme was limited by the nonlinearity of the RF driver and the phase modulator. To overcome these limitations, several methods can be employed: multiple stages of phase modulation can be used instead of a single phase modulator. Also, by using a phase conjugation technique or pre-chirping the pump, it could also be possible to suppress the chirp induced on the idler pulses.

## Acknowledgment

The authors thank Thibaut Sylvestre from Femto-ST Institute for the loan of the HNLF fiber. The authors also thank Kishi Naoto for fruitful discussions.